Inorganic Chemistry

Article

Synthesis and Mesogenic Properties of Binuclear Copper(II) Complexes Derived from Salicylaldimine Schiff Bases

Reinhard Paschke,[†] Stefan Liebsch,[†] Carsten Tschierske,[‡] Michael A. Oakley,[§] and Ekkehard Sinn*,[∥]

BioCentre, Martin Luther University Halle-Wittenberg, 06099 Halle, Germany, Department of Chemistry, Martin Luther University Halle-Wittenberg, 06099 Halle, Germany, Croda Universal, Oak Road, Hull HU6 7PH, U.K., and Department of Chemistry, University of Missouri–Rolla, Rolla, Missouri 65409

The synthesis and mesomorphic (liquid crystal) properties of new binuclear dihalocopper(II) complexes derived from N- and ring-substituted salicylaldimine Schiff bases are reported, together with the mesomorphic properties of their monomeric precursor complexes. With just N-substituents both the dichlorodicopper(II) binuclear complexes and their mononuclear analogues are waxy solids with melting points that increase with their N-chain length. However, with both N- and ring-substituents in the 4-positions, the mononuclear and binuclear complexes are each liquid crystalline or *mesogenic*, except in case of the mononuclear complexes where the N-substituent is straight chain alkyl. The other mononuclear complexes exhibit a variety of liquid crystal phases: smectic A, C, and E (S_A, S_C, and S_E, respectively). The liquid crystal phase S_A is observed in the binuclears with shorter chain N-substituents p-R–O–C$_6$H$_4$– and shorter chain ring-substituents. The chain lengths were increased until the phase behavior expanded to a further form S_C in the case of an N-substituent p-C$_{14}$H$_{29}$O–C$_6$H$_4$– and a –OC$_{12}$H$_{25}$ ring substituent. This points the way toward achieving multiphase behavior with these binuclear systems. The Cu–Br analogues of the binuclear complexes behave similarly but with significant qualitative differences, specifically lower mesophase stability and higher melting temperatures. The structures of the nonmesogenic binuclears ([Cu(*N*-dodecylSal)X]$_2$, X = Cl, Br) were determined with the aid of X-ray crystallography. These are prototypes for the structures of the binuclear complexes and especially for the shape of the central Cu$_2$O$_2$ X$_2$ core in the binuclears: distorted planar coordination about the copper with distortion toward tetrahedral measured by a characteristic twist angle τ (0° planar; 90° tetrahedral). The binuclear complexes also show magnetic coupling which can be used to estimate the geometry. For [Cu(*N*-dodecylSal)X]$_2$ $\tau > 36°$, which corresponds to weaker coupling than observed in the mesogenic binuclears where a stronger magnetic coupling indicates a geometry closer to planar ($\tau = 25°$). The mesophases were characterized by differential scanning calorimetry (DSC) analysis and optical polarized microscopy.

Introduction

Compounds that combine the properties of liquid crystals (mesogens) with those of transition metals are an attractive target of chemical research and have led to a wide variety of structural types, incorporating a wide range of metals.[1,2]

Transition metal complexes not only afford new pathways to unusual geometries but their properties are conducive to the production of compounds with unique features such as high birefringence, polarizability, paramagnetism, and color. New approaches by several groups use metal complexes for, e.g., photopolymerization,[2] the generation of blue phases,[3] and ionically conducting nanocomposite materials.[4] Research

* Author to whom correspondence should be addressed. E-mail: esinn@umr.edu.
† BioCentre, Martin Luther University Halle-Wittenberg.
‡ Department of Chemistry, Martin Luther University Halle-Wittenberg.
§ Croda Universal.
∥ University of Missouri–Rolla.

(1) Giroud-Godquin, A. M. In *Handbook of Liquid Crystals*; Demus, D., Goodby, J. W., Gray, G. W., Spiess, H. W., Vill, V., Eds.; Wiley-VCH Verlag GmbH: Weinheim, Germany, 1998; Vol. 1, p 901.
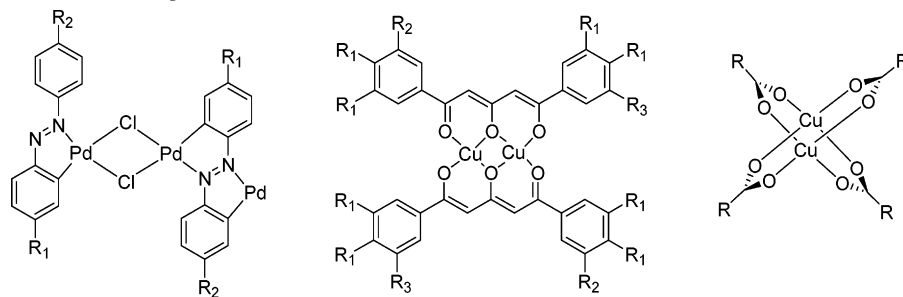
(2) Cano, M.; Oriol, L.; Pinol, M.; Serrano, J. L. *Chem. Mater.* **1999**, *11*, 94.

(3) Buey, J.; Espinet, P.; Kitzerow, H. S.; Strauss, J. *Chem. Commun.* **1999**, 441.

(4) Dag, O.; Verma, A.; Ozin, G. A.; Kresge, C. T. *J. Mater. Chem.* **1999**, *9*, 1475.
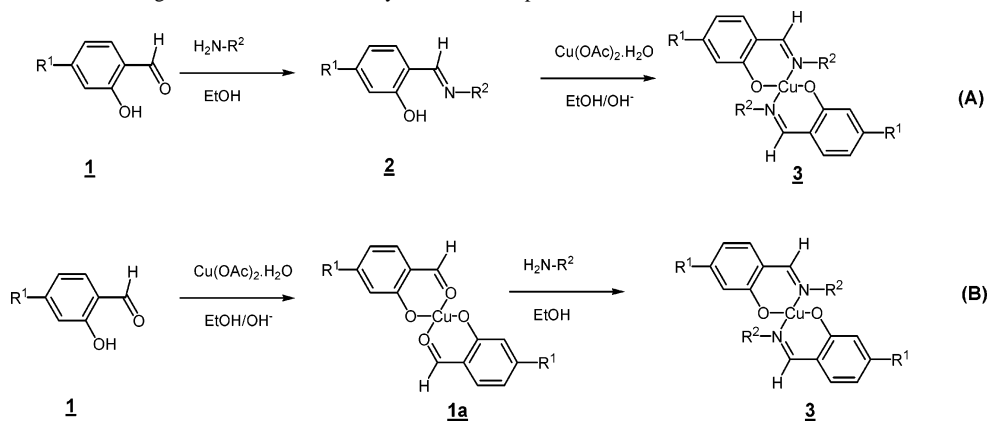
Binuclear Copper(II) Complexes

Scheme 1. Examples for Binuclear Complexes[a]

[a] Left to right: dinuclear azopalladium(II) complex,[13] alkoxy-substituted bis(1,5-diphenyl-1,3,5-pentanetrionato)dicopper(II) complex,[14] and dinuclear tetraalkanoate−copper(II) complex.[15]

Scheme 2. Synthetic Route to Ring- and N-Substituted Salicylaldimine Complexes **3**

on metallomesogens is dominated by mononuclear complexes, but introducing further metal centers could lead to very interesting effects such as ferromagnetism, antiferromagnetism, or mixed oxidation states from which new magnetic or electronic behavior and materials may arise. Although a variety of binuclear complexes are known, the search for new geometries and structures is still a challenging goal for chemists.[5−11] Binuclear mesogen complexes are still limited mainly to copper carboxylates and dithiocarboxylates, ortho- or cyclopalladated compounds, and dicopper β-diketonate and β-enaminoketonate complexes.[12] Examples for the structures of binuclear complexes are given in Scheme 1.

Polynuclear complexes have intermetallic distances ranging from very large, e.g., 6.524 Å and 17.802 Å in the same molecule,[16] to very small, e.g., 2.17 Å with metal−metal

bonding,[17] or the distance can be intermediate, at around 3.0 Å with bridging ligand atoms linking the metals.[18] It is also the intermediate metal−metal separations that lead to the most magnetic coupling. In magnetically nondilute complexes, the electronic structure, as revealed by magnetic coupling, is determined by molecular structure, so magnetic measurements can be key in structure elucidation. Even over long distances, e.g., a 10 Å pathway,[19] the metals in binuclear Cu^{II} complexes can show magnetic coupling. The ability to control the location and orientation of transition metals in multinuclear complexes allows the design of new materials with useful magnetic and electronic properties.[20−24] Our approach uses the conversion of mononuclear salicylaldimine

(5) Benouazzanne, M.; Coco, S.; Espinet, P. *Inorg. Chem.* **2002**, *41*, 5754−5759.

(6) Espinet, P.; Etxebarria, J.; Marcos, M.; Perez-Jubindo, M. A.; Ros, M. B.; Serrano, J. L. *Mater. Res. Soc. Symp. Proc.* **1995**, *392*, 123.

(7) Ghedini, M.; Pucci, D.; Crispini, A.; Aiello, I.; Barigelletti, F.; Gessi, A.; Franceescangeli, O. *Appl. Organomet. Chem.* **1999**, *13*, 565.

(8) Lydon, D. P.; Cave, G. W. V.; Rourke, J. P. *J. Mater. Chem.* **1997**, *7*, 403.

(9) Neumann, B.; Hegmann, T.; Wolf, R.; Tschierske, C. *Chem. Commun.* **1998**, 105.

(10) Lai, C. K.; Lin, R.; Lu, M. Y.; Kao, K. C. *J. Chem. Soc.* **1998**, 1857.

(11) Lai, C. K.; Leu, Y. F. *Liq. Cryst.* **1998**, *25*, 689.

(12) Serrano, J. L. *Metallomesogens: Synthesis, Properties, and Applications*; VCH Verlagsgesellschaft mbH: Weinheim, 1996; p 498.

(13) Ghedini, M.; Longeri, M.; Bartiolino, R *Mol. Cryst. Liq. Cryst.* **1982**, *84*, 207−211

(14) Serrette, A. G.; Lai, C. K.;. Swager, T. M. *Chem. Mater.* **1994**, *6*, 2252.

(15) Grant, R. F. *Can. J. Chem.* **1964**, *42*, 951.

(16) Lloris, J. M., Martínez-Mánez, R.; Padilla-Tosta, M. E.; Pardo, T.; Soto, J.; Garcia-España, E.; Ramírez, J. A.; Burgete, S. V.; Luis, S. V.; Sinn. E. *J. Chem. Soc., Dalton Trans.* **1999**, 1779.

(17) Kenny, J. P.; King, R. B.; Schaefer, H. F., III. *Inorg. Chem.* **2001**, *40*, 900.

(18) Eguchia, S.; Nozaki, T.; Miyasaka, H.; Matsumoto, N.; Okawa, H.; Kohata, S.; HoshinoMiyajima, N. *J. Chem. Soc., Dalton Trans.* **1996**, 1761.

(19) Szydłowska, J.; Krówczyński, A.; Górecka, E.; Pociecha, D. *Inorg. Chem.* **2000**, *39*, 4879.

(20) Nanda, K. K.; Addison, A. W.; Sinn, E.; Thompson L. K. *Inorg. Chem.* **1996**, *35*, 5966.

(21) Blake, A. B.; Sinn, E.; Yavari, A.; Moubaraki, B.; Murray, K. S. *Inorg. Chim. Acta* **1995**, *229*, 281.

(22) Sinn, E. *J. Chem. Soc., Chem. Commun.* **1975**, 665. Davis, J. A.; Sinn, E. *J. Chem. Soc., Dalton Trans.* **1976**, 165 and references therein.

(23) Butcher, R. J.; Overman, J. W.; Sinn, E. *J. Am. Chem. Soc.* **1980**, *102*, 3276.

(24) Magnetic Properties. Sinn, E. In *Encyclopaedia of Analytical Chemistry*; Townshend, A., Ed.; Academic Press: New York, 1995; pp 2765−2780 and references therein.

complexes of type **3** (Scheme 2) with metal halides to obtain suitable dicopper complexes.[22–24]

Complexes **3** can be prepared via two different routes. The selection of the method depends on the intended substitution pattern and the relative solubilities of **1a** and **2**. Scheme 3 shows the binucleation for a chloro complex of type **4**.[22–24] The analogous dibromodicopper(II) complexes **4b** are prepared similarly.

Experimental Section

General. All solvents were purified and dried by standard procedures. C, H, N and Cl, Br analyses were carried out on a Carlo Erba 1102, a Leco CHNS-932 microanalyzer, and a Fisons Instruments EA 1108 CHN elemental analyzer, and by Galbraith plc. ^{1}H NMR spectra were recorded on a Bruker WP 200 and a Varian Unity 500 with TMS as an internal standard. UV−vis spectra were recorded on a Perkin-Elmer Lambda 19. IR absorption spectra were measured using a FT-IR-Spectrum 1000 Perkin-Elmer, a Perkin-Elmer 983G infrared spectrometer, and a Perkin-Elmer 882 infrared spectrometer. The textures and mesophases were studied with an optical microscope "OPTIPHOT-2" (NIKON) equipped with polarized light and a Linkham hotstage TMH 600/S. Measurements of transition temperatures were carried out using a Perkin-Elmer DSC-7 calorimeter with a heating or cooling rate of 10 °C/min. 4-*n*-Alkyloxy-2-hydroxybenzaldehydes were obtained according to literature methods.[1]

Synthesis of the 4-*n*-Alkyloxy-2-hydroxybenzaldimines 2. To a stirred solution of 5 mmol 4-*n*-alkyloxy-2-hydroxybenzaldehyde, **1**, in 20 mL ethanol were added a trace of *p*-toluensulfonic acid, a drop of acetic acid, and an equimolar amount of the amine diluted with 20 mL of ethanol. The solution was refluxed for 30 min. The yellow solid was filtered off and recrystallized from methanol (average yield 60%) (example below).

N-*p*-*n*-Decyloxyphenyl-4-*n*-decyloxy-2-hydroxybenzaldimine. Anal. Found: C 77.34, H 10.42, N 2.89%. Calcd for $C_{33}H_{51}NO_3$ (MW = 509.7): C 77.75, H 10.08, N 2.75%. ^{1}H NMR (CDCl$_3$, 270 MHz): $\delta = 0.9$ (t, 6 H, 2 CH$_3$), 1.2−1.8 (m, 32 H, Alkyl-CH$_2$), 6.45 (d, 2 H, Aryl-H), 6.9 (d, 2 H, Aryl-H), 7.3 (m, 3 H, Aryl-H), 8.5 (s, 1 H, −CH=N−), 13.9 (s, 1 H, Ar−OH). IR (KBr (cm^{-1})): 2920 (s), 2840 (s), 1620 (s), 1510 (m, s), 1470 (m, s), 1290 (m), 1250 (s), 1190 (m), 1045 (m), 830 (s) 720 (w), 540 (w). Cr 75 S$_A$ 127 I.

Synthesis of the Substituted Bis(salicylaldimine)copper(II) Complexes 3. To a stirred solution of 2.5 mmol of the 4-substituted salicylaldimine **2** in 30 mL warm ethanol was added a solution of 1.25 mmol Cu(OAc)$_2$·H$_2$O in 20 mL of hot methanol or ethanol/H$_2$O (1:1). The mixture was refluxed for another 30 min. The complexes precipitating from the solution can be recrystallized from methanol/CH$_2$Cl$_2$ (yield 50−80%) (example **3.22** below).

Bis[(N-*n*-dodecyl)(4-dodecyloxysalicylaldimine]copper(II) 3.22. IR (KBr (cm^{-1})): 3448 (s), 2919 (s), 2851 (s), 1621 (s), 1530 (m), 1469 (m), 1442 (w), 1397 (m), 1322 (m), 1242 (w), 1178 (m), 1145 (m), 1028 (w), 841 (w), 774 (m), 719 (w). 604 (w), UV (nm): 264, 298, 361.

Bis(N-*n*-dodecylsalicylaldimine)copper(ii) 3.25. Salicylaldehyde (0.5 cm^3, 0.61 g, 5.0 mmol) was dissolved in methanol (10 cm^3), and 1-aminododecane (0.9 cm^3, 0.59 g, 10.00 mmol) was added. After a few minutes the Schiff base precipitated as yellow plates. Dichloromethane was added until the solid dissolved. This solution was added slowly with stirring to a solution of copper(ii) acetate monohydrate (0.50 g, 2.50 mmol) in hot methanol (50 cm^3). Sodium acetate trihydrate (0.40 g) and sodium hydroxide (0.20 g)

Table 1. Xray Crystallographic Parameters for Dichlorobis(*N*-*n*-dodecylsalicylaldimine)dicopper(II), **4.25a**, and Dibromobis(*N*-*n*-dodecylsalicylaldimine)dicopper(II), **4.25b**

	4.25a	**4.25b**
formula, fw	[CuClONC$_{19}$H$_{30}$]$_2$, 774.90	[CuBrONC$_{19}$H$_{30}$]$_2$, 863.80
crystal dimens/mm	0.380 × 0.350 × 0.230	0.340 × 0.280 × 0.230
cell params		
a/Å	7.848(3)	7.924(3)
b/Å	18.043(3)	18.064(7)
c/Å	7.724(4)	7.830(3)
α/deg	93.36(3)	92.79(4)
β/deg	116.32(3)	116.64(8)
γ/deg	97.60 (3)	98.06(3)
V/Å^3	963(1)	984(2)
space group, *Z*	P$\bar{1}$ (No. 2), 1	P$\bar{1}$ (No. 2), 1
D_{calc}/g cm^{-3}	1.336	1.457
μ(Mo Kα)	12.79	31.27
T/°C, $2\theta_{max}$/deg	23, 50.1	23, 50.1
reflns: total, unique	3690, 3417	3768, 3491
observations, undvariables	2854, 208	2066, 208
R; R_w; GOF	0.039; 0.041; 4.32	0.045; 0.045; 2.27
max, min peaks/e$^-$ Å^{-3}	0.51, −0.64	0.87, −0.65
τ/deg (Figure 2)	36.5	38.9

were added and the solution heated almost to reflux. The heat was removed and the mixture stirred (30 min) and allowed to stand (16 h). The product was filtered off, washed with water, crystallized from methanol, and dried in vacuo to yield the title compound as a brown powder (1.18 g, 73%).

Synthesis of the 4-Substituted Bis[halogeno(*N*-subst(ring-subst-2-hydroxybenzylidene)amine-(*N*,*μ*-*O*)-copper(II)] Complexes, 4 (Chloro) and 4b (Bromo). To a stirred and refluxed solution of 0.5 mmol of the appropriate bis[*N*-aryl(salicyladimine)-copper(II)] complex **3** in 15 mL ethanol was added chloroform dropwise until the solid dissolved completely. To form the chloro or bromo complexes, a concentrated ethanolic solution of 0.128 g (0.75 mmol) CuCl$_2$·2H$_2$O or 0.168 g (0.75 mmol) CuBr$_2$, respectively, was added and the reaction mixture was refluxed for another 15 min. After evaporation of one-third of the solvent and allowing the solution to stand for some days the resulting green solid was filtered off, washed with diethyl ether, and dried under vacuum (yield 20−50%) (example **4.22** below).

Dichlorobis(N-*n*-dodecyl-4-decylsalicylaldimine)dicopper-(II) 4.22. IR (KBr/cm^{-1}): 3449 (s), 2922 (s), 2852 (s), 1618 (m), 1551 (w), 1498 (s), 1405 (w), 1361 (m), 1296 (w), 1231 (m), 1194 (m), 1125 (m), 982 (w), 826 (m), 808 (w), 721(w), 637 (w), UV (nm): 260, 300, 332.

X-ray Diffraction Crystals for Dihalobis(N-*n*-dodecylsalicylaldimine)dicopper(II) (Halo = Cl, 4.25a, and Br, 4.25b). Bis-(*N*-*n*-dodecylsalicylaldimine)copper(II) (1.00 mmol) was dissolved in methanol (20 cm^3), small portions of chloroform being added as necessary to facilitate dissolution. The appropriate copper(II) halide (anhydrous or dihydrate, 1.40 mmol) was added. The mixture was heated to reflux for 10 min, and the product crystallized either on cooling or on standing for a day. The product was filtered off as a dark brown powder, washed with methanol, and dried in vacuo. Suitable crystals for single-crystal X-ray work were chosen from the samples.

X-ray Data Collection and Processing for [Cu(N-dodecylSal)-Cl]$_2$, 4.25a, and [Cu(N-dodecylSal)Br]$_2$], 4.25b. A summary of the crystallographic data is given in Table 1. Black prismatic crystals of **4.25a** and **4.25b** mounted on glass fibers were used for unit cell and structure determination. Measurements were carried out as

previously described, using the ω-scan method on a Rigaku AFC6S diffractometer[25] with graphite monochromated Mo Kα radiation and were corrected for Lorentz−polarization effects and absorption.[26] The intensities of three representative reflections measured after every 150 reflections declined by 0.13% for **4.25a**, for which a linear correction was applied, while there was no change for **4.25b**. The metal and halogen positions for **4.25a** were determined from a 3-D Patterson function. Isomorphism was used to determine **4.25b**. This phased the data sufficiently to locate the other atoms from difference Fourier maps. Full-matrix least-squares refinement[27−33] on 2854 (**4.25a**) or 2066 (**4.25b**) reflections with $F_o^2 > 3\sigma(F_o^2)$ gave unweighted and weighted agreement factors of $R = \sum\{||F_o| - |F_c||\}/\sum|F_o| = 0.039$, $R_w = [\sum w(|F_o| - |F_c|)^2/\sum(wF_o^2)]^{1/2} = 0.041$ for **4.25a** and $R = 0.045$, $R_w = 0.045$ for **4.25b**. The weighting scheme was based on counting statistics and included a factor ($p = 0.01$) to downweight the intense reflections.

Results and Discussion

Synthesis. The starting materials for the dicopper complexes are the bis(salicylaldimine)copper(II) complexes **3** (Scheme 2) which can be prepared via two different routes (A) and (B), of which (B) is better for the production of libraries of small molecule complexes. However for the large molecules here, we preferred route (A) because of better yields and shorter reaction times. The Schiff base derivatives **2** were reacted with copper(II) acetate to produce brown or green complexes which can be recrystallized from methanol/CH$_2$Cl$_2$. The identity of the complexes was confirmed by elemental analysis and IR and UV/vis spectroscopy. The binucleation reaction is shown in Scheme 3.[34,35] In the presence of a solvent which can coordinate to copper(II) and in which the CuCl$_2$ can ionize, the binuclear complexes **4** are formed. Although the color change associated with the formation of the dicopper(II) complex occurs immediately, it can take days until the solid complex is precipitated. The rate-determining step therefore seems to be the coordination of the halide,[34] and the most likely mechanism is shown in Scheme 4.

(25) Backhouse, J. R.; Lowe, H. M.; Sinn, E.; Suzuki, S.; Woodward, S. *J. Chem. Soc., Dalton Trans.* **1995**, 1489.

(26) An empirical absorption correction, based on azimuthal scans of several reflections, was applied which resulted in transmission factors ranging from 0.89 to 1.09 for **4.25a** and 0.81 to 1.22 for **4.25b**.

(27) Least-squares: Function minimized is $\sum w(|F_o| - |F_c|)^2$ where $w = 4F_o^2/\sigma^2(F_o^2)$; $\sigma^2(F_o^2) = [S^2((C + R)2B) + (pF_o^2)^2]/Lp^2$; $S =$ scan rate; $C =$ total integrated peak count; $R =$ ratio of scan time to background counting time; $p = p$-factor; $B =$ total background count; Lp = Lorentz−polarization factor.

(28) TEXSAN−TEXRAY Structure Analysis Package, Molecular Structure Corporation, 1985.

(29) The standard deviation of an observation of unit weight ($[\sum w(|F_o| - |F_c|)^2/(N_o - N_v)]^{1/2}$ where $N_o =$ number of observations, $N_v =$ number of variables) was 208.

(30) Neutral atom scattering factors were taken from Cromer and Waber.[31] Anomalous dispersion effects were included in F_{calc};[32] the values for Δf and $\Delta f'$ were those of Cromer.[33]

(31) Cromer, D. T.; Waber, J. T. *International Tables for X-ray Crystallography*; The Kynoch Press: Birmingham, England, 1974; Vol. IV, Table 2.2 A.

(32) Ibers, J. A.; Hamilton, W. C. *Acta Crystallogr.* **1964**, *17*, 781.

(33) Cromer, D. T. *International Tables for X-ray Crystallography*; The Kynoch Press: Birmingham, England, 1974; Table 2.3.1, Vol. IV.

(34) Sinn, E.; Harris, C. M. *Coord. Chem. Rev.* **1969**, *4*, 391. Sinn, E. *Coord. Chem. Rev.* **1970**, *5*, 313 and references therein.

(35) Sinn, E. In *Biological and Inorganic Copper Chemistry*; Karlin, K. D., Zubieta, J., Eds.; Adenine Press: Guilderland, NY, 1986 and references therein.

Scheme 3. Conversion of Mononuclear Ring- and N-Substituted Salicylaldimine Complexes 3 to Dicopper Complexes
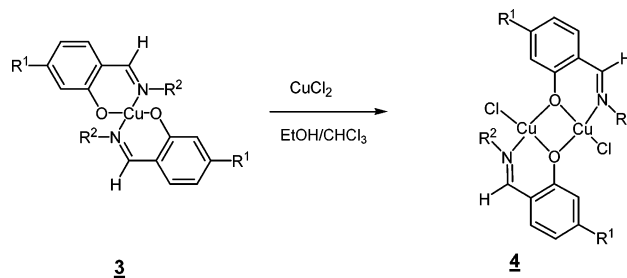
Ligand field spectroscopy and crystallography show that a trend from planar to tetrahedral stereochemistry is observed when the substituents become bulky.[22,34,36,37] This must be taken into consideration because our ligands may intensify this effect, and the metal−ligand geometry influences the nature of the liquid crystalline phases formed, and even whether liquid crystal formation occurs at all. The binuclear complexes **4** are deep green or deep red in color and insoluble in many organic solvents. The identity of the complexes was confirmed by elemental analysis, IR, and UV spectroscopy.

UV−Visible Spectra. The UV−visible spectra of the complexes **3** and **4** are similar but also show consistent changes in the charge-transfer region. The biggest change is a shift of ca. 30 nm to higher energy in the lowest energy band (e.g., 360.9 nm to 332.0 nm from mononuclear **3.22** to binuclear **4.22**; 389.1 nm to 361.3 nm from **3.10** to binuclear **4.10**).

Infrared Spectra. Although the infrared spectra of the complexes **3** and **4** have a considerable complexity, it is obvious that the conversion to the binuclear complexes leads to significant characteristic changes. The most dramatic change is the shift of the bands associated with the bridging oxygens, e.g., the band near 1530 cm^{-1}, assigned to the C−O stretching vibration for which shifts to higher energy of ca. 20 cm^{-1} result from the increased constraint introduced by the oxygen bridging.[22,34,36,37] Another indication for an increasing constraint upon the vibrations is a distinctive shift to higher energy in the bands near 1470, 1180, and 770 cm^{-1}.

Relation of Structure to Liquid Crystal Behavior and Magnetic Coupling. A view of the single molecules of both the X = Cl (**4.25a**) and X = Br (**4.25b**) forms of the binuclear [Cu(N-dodecylsalicylaldimine)X]$_2$ complexes are shown as the ORTEP[38] representation in Figure 1. The other lower melting complexes could not be crystallized readily so **4.25a** and **4.25b** were chosen as representatives of the long-chain class of binuclear complexes for X-ray crystallographic characterization.

Mononuclear (**3**) and binuclear (**4**, **4b**) complexes with R^1 = H and with long chain N-substituents, R^2, are waxy solids with melting points that increase with their N-chain length but with no mesogenic properties.[39,40] Of these the binuclears show strong intramolecular antiferromagnetic coupling like all previous examples of type **4** binuclears and

(36) Sinn, E. *Inorg. Chem.* **1976**, *15*, 358; 366; 2698.

(37) Butcher, R. J.; Sinn, E. *Inorg. Chem.* **1976**, *15*, 1604.

(38) Johnson, C. K. *ORTEPII*; Report ORNL-5138; Oak Ridge National Laboratory: Oak Ridge, TN, 1976.

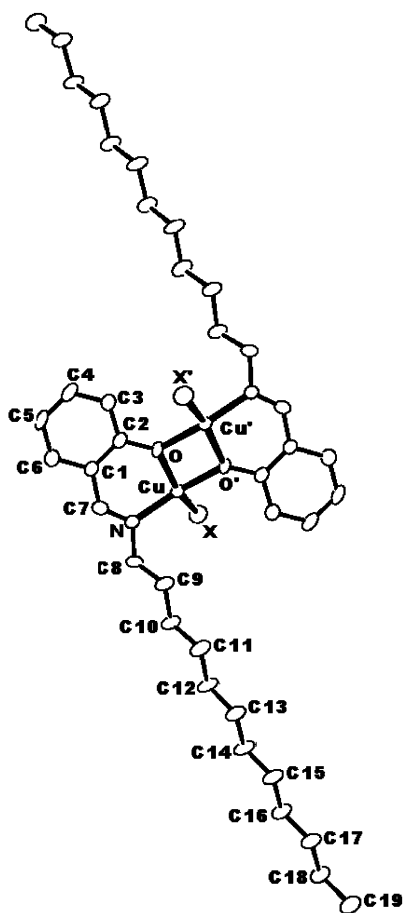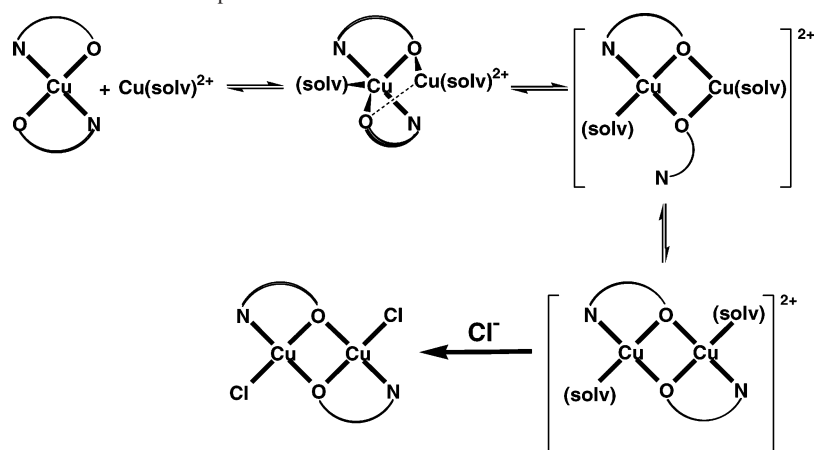**Scheme 4.** Proposed Mechanism of Binuclear Complex Formation

Figure 1. ORTEP view of [Cu(*N*-dodecylSal)Cl]$_2$, **4.25a** (X = Cl), and [Cu(*N*-dodecylSal)Br]$_2$, **4.25b** (X = Br).

Figure 2. Distortion angle τ at the coordination sphere of a binuclear complex.

magnetism and the molecular structure, and then to consider the application of this knowledge to the liquid crystal binuclears. Strong superexchange interactions lead to the signature coupling of the bridging Cu$_2$O$_2$ core in Figure 2 for all the binuclears. The magnitude ($-2J$, from the Hamiltonian $\mathscr{H} = -2J\mathbf{S}_1 \cdot \mathbf{S}_2$) is greatest for the optimal superexchange pathway at $\tau = 0$ when the d$_{x^2-y^2}$ unpaired electrons see each other through the σ bond to the aryl oxygen, and decreases with increasing τ.[24,34] The relationship holds whether X in Figure 2 is Cl (as in **4**), Br, or O, whether a ligand ring substituent is present and whether the N-substituent is aryl or short alkyl. It applies to a wide series of type **4** complexes currently under study where the spectroscopic bands again support the correlation.[39] The magnitude of the coupling ($-2J$ value of 300 cm^{-1} for the ring$-$O$-$C$_{10}$ chloro complex **4** with N$-$C$_6$H$_4$$-O-C_{10}$) calibrates the geometry about the metal atom as near planar, with a distortion angle τ of about 25°, indicating a somewhat more flattened configuration than in **4.25a**[40] ($-2J = 200$ cm^{-1} for a τ value of 36.5°).

The overall structures each resemble a ribbon or ladder with a kink in it. This is best seen in the interplanar angles. The two aryl rings in each molecule are mutually parallel (zero interplanar angle imposed by the crystallographic inversion center), but the dihedral angle between the central Cu$_2$O$_2$ bridging plane and the aryl rings is 27.9° for the chloro complex **4.25a** and 27.5° for the bromo complex **4.25a**.

Mesomorphic Properties. The ligands themselves may be mesogenic, e.g., *N-p-n*-Decyloxyphenyl-4-*n*-decyloxy-2-hydroxybenzaldimine has a smectic A range 75$-$127 °C.

Bis(salicylaldimine)copper(II) Complexes 3. Salicylaldimine complexes of the type **3** have been investigated by

their many analogues.[22,24,34,35] Also, appropriate ring- and N-substituents R^1 and R^2 lead to mesogenic properties. The binuclears therefore combine magnetic coupling and liquid crystal properties, vide infra. It therefore becomes relevant to relate the electronic structure as determined by the

(39) Liebsch, S.; Paschke, R.; Sinn, E. *Inorg. Chem. Commun.* **2002**, *5*, 525. J. R. Chipperfield, J. M. Elliott, S. Liebsch, R. Paschke, and E. Sinn. ACS 35th Midwest Regional Meeting, St Louis MO, Oct 25$-$28, 2000 (114).

(40) Oakley, M. A. Dissertation, Hull, 1995 (X-ray and other characterization data available electronically).
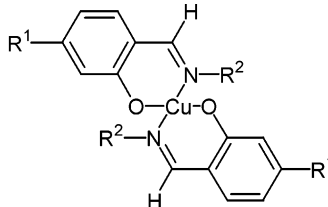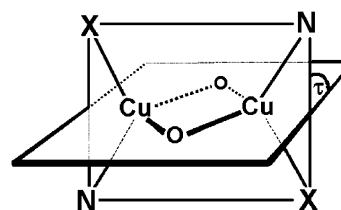
Table 2. Mesomorphic Phase Transition Temperatures (T) and Enthalpies (ΔH) for the New Mononuclear Complexes **3**, $T/°C$ [$\Delta H/$kJ mol^{-1}]

Compound	R^1	R^2	Cr_1	Cr_2	S_E	S_C	S_A	I
3.1	OC_8H_{17}	p-$C_7H_{15}O$-C_6H_4		124	136	158	165	.
3.2	OC_8H_{17}	p-$C_8H_{17}O$-C_6H_4		126	138	156	162	.
3.3	OC_8H_{17}	p-$C_{10}H_{21}O$-C_6H_4		140.6 [59.1]	-	153 [0.6]	159.4 [11.0]	.
3.4	OC_8H_{17}	p-$C_{12}H_{25}O$-C_6H_4		122 [41.7]	-	132 [0.6]	140.3 [7.7]	.
3.5	OC_8H_{17}	p-$C_{14}H_{29}O$-C_6H_4	99.7 [37.7]	121 [37.0]	-	131.9 [0.8]	145.3 [10.0]	.
3.6	OC_8H_{17}	$C_{12}H_{25}$	91.6 [28.8]	97.7 [60.9]	-	-	-	.
3.7	OC_8H_{17}	$C_{18}H_{37}$		87.8 [91.0]	-	-	-	.
3.8	OC_8H_{17}	p-C_7H_{15}-C_6H_4		145 [48.7]	-	-	147 [11.5]	.
3.9	$OC_{10}H_{21}$	p-$C_7H_{15}O$-C_6H_4		133.9 [47.8]	93) [27.3]	149 [1.2]	160 [10.9]	.
3.10	$OC_{10}H_{21}$	p-$C_8H_{17}O$-C_6H_4		134.5 [39.7]	95) [29.0]	151.7 [0.8]	156.7 [11.0]	.
3.11	$OC_{10}H_{21}$	p-$C_{10}H_{21}O$-C_6H_4		131 [39.5]	125.6) [6.4]	144	146 [8.8]	.
3.12	$OC_{10}H_{21}$	p-$C_{12}H_{25}O$-C_6H_4		134 [44.8]	-	147	151 [10.9]	.
3.13	$OC_{10}H_{21}$	p-$C_{14}H_{29}O$-C_6H_4	105.2 [21.0]	124.9 [39.4]	-	-	142 [9.8]	.
3.14	$OC_{10}H_{21}$	$C_{12}H_{25}$	95.0 [25.5]	98.9 [44.1]	-	-	-	.
3.15	$OC_{10}H_{21}$	$C_{18}H_{37}$	-	93.0	-	-	-	.
3.16	$OC_{10}H_{21}$	p-C_7H_{15}-C_6H_4	-	133	.	137	140	.
3.17	$OC_{12}H_{25}$	p-$C_7H_{15}O$-C_6H_4	93.0 [10.5]	126.4 [35.2]	-	-	157.4 [10.5]	.
3.18	$OC_{12}H_{25}$	p-$C_8H_{17}O$-C_6H_4	-	124	-	142	150	.
3.19	$OC_{12}H_{25}$	p-$C_{10}H_{21}O$-C_6H_4	-	127	-	145	147	.
3.20	$OC_{12}H_{25}$	p-$C_{12}H_{25}O$-C_6H_4	-	119	-	-	134	.
3.21	$OC_{12}H_{25}$	p-$C_{14}H_{29}O$-C_6H_4	105.8 [31.5]	122 [34.7]	(80) [26.3]		131.5 [4.1]	.
3.22	$OC_{12}H_{25}$	$C_{12}H_{25}$	74 [41.5]	94.1 [64.9]	-	-	-	.
3.23	$OC_{12}H_{25}$	$C_{18}H_{37}$	-	98 [119]	-	-	-	.
3.24	$OC_{12}H_{25}$	p-C_7H_{15}-C_6H_4	78.4 [16.9]	124.8 [25.1]	84.5 [6.0]	107) [0.2]	140.7 [11.5]	.
3.25	H	$C_{12}H_{25}$	57-59	-	-	-	-	.

many groups,[41-50] and a large number of compounds with alkyl, alkyloxy, and especially alkyloxybenzoyloxy substituents have been reported. Our series of complexes (Table 2) completes this class of substances. Of the complexes in the present study only compounds **3.11**, **3.13**, and **3.14**[51] have been previously reported. These literature results were

(41) Caruso, U.; Roviello, A.; Sirigu, A. *Liq. Cryst.* **1988**, *3*, 1515.
(42) Polishchuk, A. P.; Antipin, M. Yu.; Timofeeva, T. V.; Struchkov, Yu. T.; Galyametdinov, Yu G.; Ovchinnikov, I. V. *Kristallografiya* **1991**, *36*, 642.
(43) Galyametdinov, Y.; Ovchinnikov, I. V.; Bolotin, B. M.; Etingen, N. B.; Ivanova, G. I.; Yagfarova, L. M. *Izv. Akad. Nauk SSSR* **1984**, 2379.
(44) Ghedini, M.; Armentano, S.; Bartolino, R.; Rustichelli, F.; Torquati, G.; Kirov, N.; Petrov, M. *Mol. Cryst. Liq. Cryst.* **1987**, *15*, 1 75.
(45) Ghedini, M.; Armentano, S.; Bartolino, R.; Torquati, G.; Rustichelli, F. *Solid State Commun.* **1987**, *64*, 1191.

(46) Ghedini, M.; Armentano, S.; Bartolino, R.; Kirov, N.; Petrov, M.; Nenova, S. *J. Mol. Liq.* **1988**, *38*, 207.
(47) Marcos, M.; Romero, P.; Serrano, J. L; Bueno, C.; Cabeza, J. A.; Oro, L. A. *Mol. Cryst. Liq. Cryst.* **1989**, *167*, 123.
(48) Marcos, M.; Romero, P.; Serrano, J. L. *J. Chem. Soc.* **1989**, 1641.
(49) Marcos, M.; Romero, P.; Serrano, J. L. *Chem. Mater.* **1990**, *2*, 495.
(50) Ovchinnikov, I. V.; Galyametdinov, Y.; Ivanova, G. I.; Yagfarova, L. M. *Dokl. Akad. Nauk SSSR* **1984**, *276*, 126.
(51) Marcos, M.; Romero, P.; Serrano, J. L.; Bueno, C.; Cabeza, J. A.; Oro, L. A. *Mol. Cryst. Liq. Cryst.* **1989**, *167*, 123.

Figure 3. Polarized micrographs observed for the S_A and S_E phases of **3.21**.

carefully reexamined with the newly resynthesized complexes. We observe both qualitative and quantitative deviations from the reported phase transitions and phase behavior in the literature. For compound **3.13** Marcos et al.[51] reported the following phase changes: Cr_1 110.7 Cr_2 129.4 S_1 145.3 S_2 147.3 I, whereas we determined the phase transitions Cr_1 105.2 Cr_2 124.9 S_A 142 I (Table 2). In the case of **3.11** we have established an additional liquid crystal phase not previously discovered despite the earlier studies, a smectic E, S_E phase, which is *monotropic*, i.e., observed only on supercooling from the melt.

Examination of analogous mesogenic salicylaldimine−copper(II) complexes with wide-angle X-ray diffraction[52−54] proved that there is no significant difference from the structural features characterizing classical liquid crystals. It therefore seemed appropiate to study the liquid crystalline behavior of all complexes **3** and **4** by thermal analysis (DSC)

and polarizing microscopy. The phase transitions and thermodynamic data for the mononuclear N- and/or ring-substituted salicylaldimine copper(II) complexes are summarized in Table 2. The behavior of all but the *N*-alkyl substituted mononuclear bis(salicylaldimine)copper(II) complexes **3** is *enantiotropic*, which means that they are liquid crystalline above their melting points. Representatives with shorter alkyloxy chains show smectic A, C, and E (S_A, S_C, and S_E) phases whereas longer chain substituents cause a loss of the S_E and S_C phases. Although in some cases pseudoisotropic S_A phases occur, the compounds usually show the typical textures for the corresponding phases. This is illustrated by Figure 3, which shows polarized micrographs observed for the S_A and S_E phases of **3.21** (substituent $OC_{12}H_{25}$ on the ring 4-position and substituent p-$C_{14}H_{29}O-C_6H_4$ on the imine nitrogen). The *N*-alkyl substituted

(52) Barbera, J.; Levelut, A. M.; Marcos, M.; Romero, P.; Serrano, J. L. *Liq. Cryst.* **1991**, *10*, 119.

(53) Borchers, B.; Haase, W. *Mol. Cryst. Liq. Cryst.* **1991**, *209*, 319.
(54) Tian, Y.; Su, F.; Xing, P.: Zhao, Y.; Tang, X.; Zhao, X.; Zhou, E. *Liq. Cryst.* **1996**, *20*, 139.

Table 3. Mesomorphic Phase Transition Temperatures (T) and Enthalpies (ΔH) for the New Binuclear Chloro Complexes **4**, T/ °C [ΔH/kJ mol^{-1}]
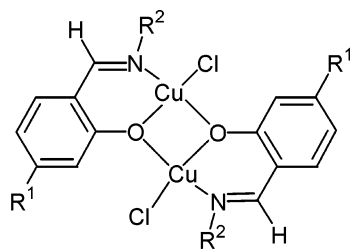
Compound	R^1	R^2	Cr_1	Cr_2	S_C	S_A	I
4.3	OC_8H_{17}	p-$C_{10}H_{21}$O- C_6H_4		73 [23.7]	-	132 [2.9]	.
4.4	OC_8H_{17}	p-$C_{12}H_{25}$O- C_6H_4		124 [19.5]	-	144.4 [5.2]	.
4.5	OC_8H_{17}	p-$C_{14}H_{29}$O- C_6H_4		78.5 [35.2]	-	132 [2.1]	.
4.6	OC_8H_{17}	$C_{12}H_{25}$		119.7 [43.8]	-	(92) [3.1]	.
4.7	OC_8H_{17}	$C_{18}H_{37}$		122 [51.4]	-	(96)	.
4.8	OC_8H_{17}	p-C_7H_{15}- C_6H_4		118.9 [30.6]	-	130.8 [9.8]	.
4.9	$OC_{10}H_{21}$	p-C_7H_{15}O- C_6H_4		86 [9.8]	-	130 [4.5]	.
4.10	$OC_{10}H_{21}$	p-C_8H_{17}O- C_6H_4		85 [6.5]	-	128 [5.5]	.
4.11	$OC_{10}H_{21}$	p-$C_{10}H_{21}$O- C_6H_4		91 [10.5]	-	125 [6.5]	.
4.12	$OC_{10}H_{21}$	p-$C_{12}H_{25}$O- C_6H_4		81.9 [26.8]	-	127.2 [3.9]	.
4.13	$OC_{10}H_{21}$	p-$C_{14}H_{29}$O- C_6H_4		84.5 [27.8]	-	123.7 [5.5]	.
4.14	$OC_{10}H_{21}$	$C_{12}H_{25}$	51.9 [14.5]	121.4 [61]	-	128.3 [9.3]	.
4.15	$OC_{10}H_{21}$	$C_{18}H_{37}$	-	109 [39.0]	-	(102) [2.0]	.
4.17	$OC_{12}H_{25}$	p-C_7H_{15}O- C_6H_4	-	93.4 [16.5]	-	126.7 [1.5]	.
4.18	$OC_{12}H_{25}$	p-C_8H_{17}O- C_6H_4	-	103	-	129	.
4.19	$OC_{12}H_{25}$	p-$C_{10}H_{21}$O- C_6H_4	-	95	-	127	.
4.20	$OC_{12}H_{25}$	p-$C_{12}H_{25}$O- C_6H_4	-	94	-	130	.
4.21	$OC_{12}H_{25}$	p-$C_{14}H_{29}$O-C_6H_4	-	104 [59.1]	115. 2 [3.7]	135.8 [7.3]	.
4.22	$OC_{12}H_{25}$	$C_{12}H_{25}$	-	120 [49.2]	-	94	.
4.23	$OC_{12}H_{25}$	$C_{18}H_{37}$	-	110 [43.7]	-	95	.
4.24	$OC_{12}H_{25}$	p-C_7H_{15}- C_6H_4	78.2 [11.4]	112.4 [13.2]	-	133.5 [34]	.
4.25a	H	$C_{12}H_{25}$	134	-	-	-	.

complexes (**3.6**, **3.7**, **3.14**, **3.15**, **3.22**, **3.23**) exhibit no mesomorphism at all.

Binuclear Complexes 4. Table 3 summarizes the phase transitions and thermodynamic data for the binuclear N- and/ or ring-substituted salicylaldimine dichlorodicopper(II) complexes **4**. Since some of the complexes crystallized only partially, the DSC values for the melting points of some compounds **4** are lower than expected. In each case for the binuclears with shorter chain N-substituents p-R−O−C$_6$H$_4$− and shorter chain ring substituents, the only liquid crystal phase observed is S$_A$. In a search for the possibility of additional phases, the ring and N-substituent alkyl chain lengths were increased until the phase behavior expanded to include an additional form, S$_C$. This occurs in complex **4.21** where the N-substituent is p-C$_{14}$H$_{29}$O−C$_6$H$_4$− and the ring-substituent is −OC$_{12}$H$_{25}$, the longest chain N- and ring-

Figure 4. Polarized micrographs observed for the S_C phase of the binuclear **4.21** ($R^1 = OC_{12}H_{25}$, $R^2 = p\text{-}C_{14}H_{29}O\text{-}C_6H_4$).

substituents in the series. A polarized photomicrograph of the new S_C phase is shown in Figure 4. This result points the way toward getting multiphase behavior with these dichlorodicopper(II) binuclear systems: the use of still longer chain substituents can promote the production of new phases.

The textures of analogous phases (S_A, S_C) in the mononuclear complexes **3** and the binuclears **4** exhibit analogical appearance, indicating very similar anisotropism of the molecular geometry. Despite the differences in molecular shape between the mono- and binuclears, both sets of molecules form layers. The wider binuclears **4** do not form a columnar ("discotic") phase; this is analogous to observations with some Pd dimers, vide infra.[55] In addition to showing only the S_A phase, most type **4** binuclear complexes (i.e., all but **4.21** discussed above) have a lowered mesophase stability compared to that of the mononuclear complexes **3** (Figure 5).

Elongation of the alkyloxy chains affects clearing and melting temperatures to a lesser extent than in the case of the mononuclear compounds **3**. The chemical stability is also diminished compared to the mononuclear complexes **3**. Both effects can be explained by the differences in chemical structure. While the increased length-to-breadth ratio and the already mentioned trend to go from partially tetrahedral to planar stereochemistry influence the mesophase stability of the binuclears **4**, the weaker Cl–Cu bond causes the lower

chemical stability. It is therefore fairly surprising that the binuclear N-alkyl-substituted complexes **4.6**, **4.7**, **4.14**, **4.15**, **4.22**, and **4.23** exhibit monotropic and enantiotropic liquid crystalline behavior, while the monomeric precursors (**3.6**, **3.7**, **3.14**, **3.15**, **3.22**, and **3.23**) do not. This was also found for dinuclear ortho-palladated 4-alkyl-4′-alkoxyazobenene-complexes[55] and emphasizes the quality of the anisotropic molecular architecture of those binuclear complexes.

Bromo Complexes 4b. Table 4 summarizes the phase transitions for the binuclear N- and/or ring-substituted salicylaldimine dibromodicopper(II) complexes **4b**. Although the bromo analogues **4b**, of the complexes **4** above, show qualitatively similar phase behavior to those of the chloro complexes, there are significant quantitative differences. The mesophase stability of the bromo complexes is lowered whereas their melting temperatures are higher (Figure 6). As in the case of the dichlorodicopper(II) complexes **4**, the textures of analogous phases (S_A) in the mononuclear complexes **3** and in their dibromodicopper(II) binuclear derivatives **4b** exhibited the same appearance, again indicating very similar mechanisms of formation of the mesophases in the monomers and the bromo binuclears. It remains true for the bromo binuclears **4b** that, regardless of the difference in molecular shapes between **4b** and those of their monomeric precursors, the molecules prefer to form layers in each case, and at least for the complexes studied there is no indication of a columnar ("discotic") phase. The less stable dibromodicopper(II) complexes were not investigated to the same detail, and therefore, although their chain length dependent behavior is similar to that of their chloro analogues, we can only speculate that sufficiently increasing the N- and ring-substituent chain lengths would also result in additional liquid crystal phases.

Conclusions

We have shown that it is possible to transform liquid crystalline bis(salicylaldimine)copper(II) complexes **3** into the corresponding binuclear copper(II) complexes **4** which also exhibit mesophases, and which in some cases have mesophases even when the parent complexes do not. The introduction of a central core which consists of the binuclear copper(II) unit deeply influences the molecular architecture. The greater length-to-breadth ratio of complex **4.6** than of **3.6** is shown schematically in Figure 7.

It cannot be taken for granted a priori that the new binuclear structures would still be able to form mesophases, and it is also conceivable that there would be a complete loss of mesophase behavior.

In case of the ortho-palladated binuclear complexes a brick-like or sanidic geometry was proposed to explain the formation of mesophases.[56] From X-ray investigation we can conclude that the new binuclear structures act as "bricks" after reaching the melting point and that this anisotropy of the structure causes the formation of smectic layers. In suitable cases, with appropriate ring-substitutions, crossovers to a columnar ("discotic") phase can be realized.[57-59]

(55) Ghedini, M.; Armentano, S.; Neve, F.; Licoccia, S. *J. Chem. Soc., Dalton Trans*. **1988**, 1565
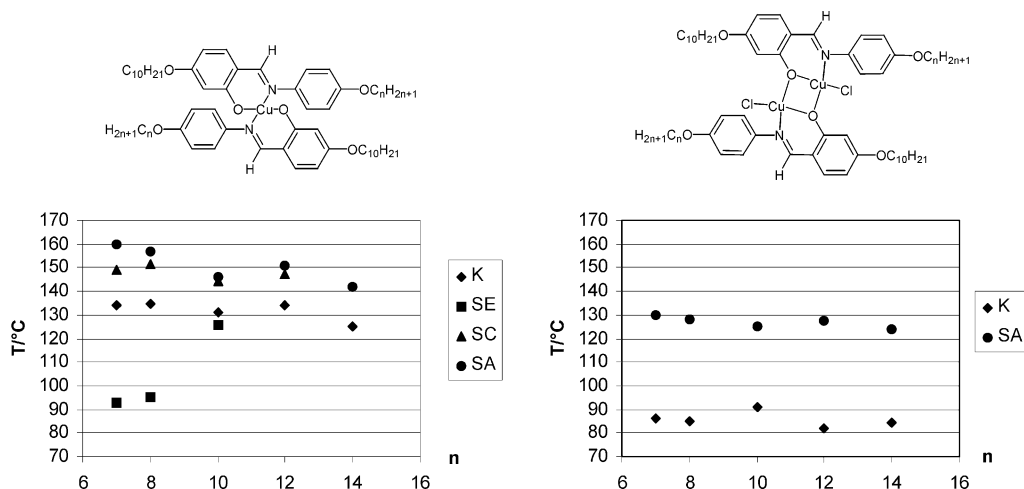
(56) Demus, D. *Liq. Cryst*. **1989**, 75.

Figure 5. Mesophase behavior of the mono- and binuclear complexes **3** and **4** with ring-substituent fixed ($-OC_{10}H_{21}$), as a function of the chain length n in the N-substituent p-$C_nH_{2n-1}O-C_6H_4-$.
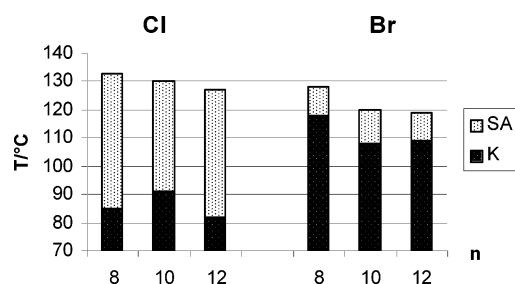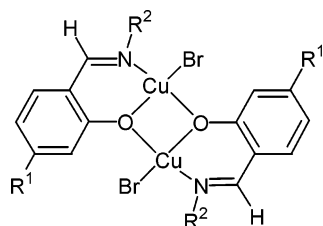

Figure 6. Mesophase behavior of the chloro complexes **4** in comparison to the corresponding bromo complexes.

Table 4. Mesomorphic Phase Transition Temperatures (T) for the New Binuclear Bromo Complexes **4b**, T/°C

Compound	R^1	R^2	Cr	S_A	I
4.10b	$OC_{10}H_{21}$	p-$C_8H_{17}O$- C_6H_4	118	128	.
4.11b	$OC_{10}H_{21}$	p-$C_{10}H_{21}O$- C_6H_4	108	120	.
4.12b	$OC_{10}H_{21}$	p-$C_{12}H_{25}O$- C_6H_4	109	119	.
4.25b	H	$C_{12}H_{25}$	107	-	.

The central core of the binuclear complexes **4**, especially the additional copper(II) and the chloro ligand, markedly increases the polarity of that region and introduces additional van der Waals and dipole interactions. This leads to an improved segregation of the alkyl chains. Evidently the greater length-to-breadth ratio is no hindrance for the formation of mesophases.

The distortion of the planar geometry in complexes **4** causes a lowering of the mesophase stability and a decrease
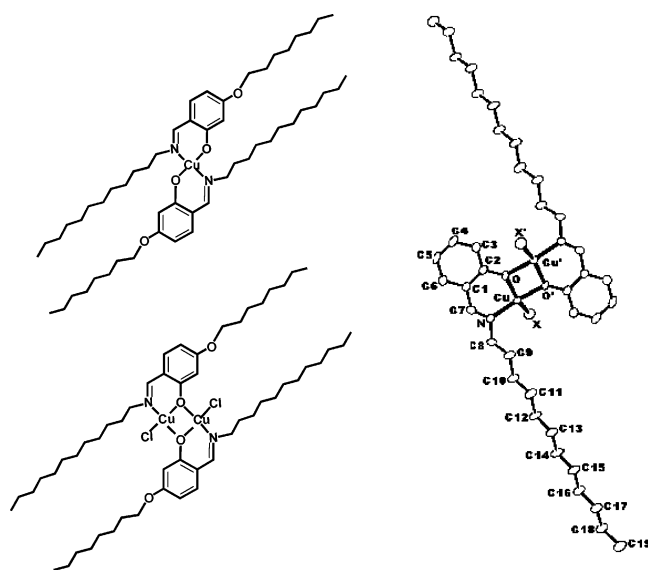
(57) Elliott, J. M.; Chipperfield, J. R.; Clark, S.; Sinn, E. *Inorg. Chem.* **2001**, *40*, 6390.
(58) Elliott, J. M.; Chipperfield, J. R.; Clark, S.; Sinn, E. *Inorg. Chem. Commun.* **2002**, *5*, 99.

Figure 7. Models of the mononuclear and binuclear complexes **3.6** and **4.6** (left) in comparison to the X-ray structure of the binuclear complex **4.25a** (right). Different length-to-breadth ratio leads to rodlike and sanidic molecular shapes.

of the melting temperatures. No liquid crystal behavior is observed in the mononuclear complexes which have straight chain alkyl N-substituents. This applies specifically to the complexes **3.6**, **3.7**, **3.14**, **3.15**, **3.22**, **3.23,** and **3.25**; DSC measurements do show that **3.6**, **3.14,** and **3.22** undergo solid state to solid state phase changes (designated $Cr_1 \rightarrow Cr_2$ in Table 2), but these are not important here and in any case could not be interpreted further without crystal structure determinations of both solid phases. The surprising fact that the ring-substituted-*N*-alkyl-substituted complexes **3** exhibit no mesomorphism at all, whereas the corresponding binuclears **4** exhibit at least monotropic behavior where at least one liquid crystal phase occurs upon supercooling from the melt, demonstrates the remarkable capability of those ribbonlike structures to form anisotropic phases.

The alkyl substituents in complexes **3** cannot maintain the necessary rigidity of the rod which is a prerequisite for the

(59) Paschke, R.; Balkow, D.; Sinn, E. *Inorg. Chem.* **2002**, *41*, 1949.

formation of the liquid crystalline state. The ribbonlike (sanidic) architecture of complexes **4** seems to provide more stability, and this is the presumed reason for their observed liquid crystal properties when none are observed in some of their mononuclear counterparts.

The new binuclear structures enhance materials chemistry in the area of binuclear metallomesogens.

For all future applications of the field of metallomesogens, it is important to draw from a wide range of compounds and classes of substances, in order to optimize the criteria for selecting appropriate materials. Since future priorities for the properties cannot yet be foreseen, founding new classes of materials remains of high importance.

It is in this context that we view our work in this area.

Supporting Information Available: Tables of microanalytical and crystallographic data. This material is available free of charge via the Internet at http://pubs.acs.org.

IC0301021